



## Synthesis of Polymers and Nanoparticles Bearing Polystyrene Sulfonate Brushes for Chemokine Binding

Naatasha Isahak<sup>a</sup>, Julie Sanchez<sup>b</sup>, Sébastien Perrier,<sup>a,c,d</sup> Martin J. Stone<sup>b</sup> and Richard J. Payne<sup>a\*</sup>

Received 00th January 20xx,  
Accepted 00th January 20xx

DOI: 10.1039/x0xx00000x

www.rsc.org/

The movement of leukocytes to the site of inflammation in response to injury or infection is orchestrated by chemokines binding and signaling through cognate receptors. The interaction between sulfated tyrosine residues on the flexible N-terminal tail of the receptor with positively charged regions of the chemokine is one of the key recognition features that facilitates binding. In this manuscript we describe the synthesis of polymers and silica nanoparticles bearing polystyrene sulfonate brushes to mimic the sulfated tyrosine residues. We show that both the polymers and nanoparticles possess high binding affinity for the chemokine monocyte chemoattractant protein-1 (MCP-1) in monomeric and dimeric form. We also demonstrate key differences in the relative affinity for the chemokine for the free polymer versus the polymer-derived nanoparticle system.

### Introduction

A hallmark of inflammation is the accumulation of leukocytes (white blood cells) in tissues in response to injury or infection. Whilst leukocytes play a critical role in neutralising infectious agents and in tissue repair, excessive leukocyte recruitment gives rise to a host of inflammatory diseases. Leukocyte trafficking in inflammation is regulated by chemokines (small, soluble proteins that are secreted from tissues in response to initial inflammatory signals) and their interactions with chemokine receptors (G protein-coupled receptors, GPCRs) that are located in the leukocyte cell membrane.<sup>1</sup> In addition to their important roles in inflammation, chemokine receptors also play important roles in cancer metastasis<sup>2</sup> and serve as important mediators of infection of cells with human immunodeficiency virus-1 (HIV-1) and the malarial parasite *Plasmodium vivax*.<sup>3,4</sup>

Inhibition of specific interactions with a given chemokine receptor represents an attractive therapeutic approach to suppress an inflammatory disease without decreasing the body's general defense against invading pathogens.<sup>5,6</sup> To date, a number of antagonists have been developed as anti-inflammatory agents.<sup>7</sup> In a similar manner chemokine receptors have also been targeted for the development of 'entry inhibitors' for the treatment of HIV.<sup>8-10</sup>

An alternative approach to ameliorate the interaction between chemokines and their receptors is to develop molecules that bind and target the chemokines themselves. This approach has recently been validated through the development of anti-chemokine monoclonal antibodies.<sup>11-14</sup>

Chemokine function is regulated by numerous factors including dimerisation, binding to cell-surface glycosaminoglycans (GAGs), proteolytic processing and site-specific post-translational modifications. We and others have characterised key recognition features of chemokines by their cognate receptors.<sup>15-24</sup> Based on this work it is now established that the flexible N-terminal extracellular tail of the receptor is a primary site for chemokine recognition and binding.<sup>22,25</sup> In many of the chemokine receptors studied to date, this N-terminal tail contains two or more Tyr residues that can undergo post-translational sulfation to generate a sulfate monoester functionality on the phenolic side chain of the amino acid.<sup>22</sup> The sulfation of tyrosine residues on the N-terminus is catalysed in the Golgi apparatus by tyrosylprotein sulfotransferase (TPST) enzymes, which preferentially sulfate tyrosine residues located near acidic residues,<sup>26</sup> a motif found in the amino terminal regions of most chemokine receptors.<sup>22,27</sup> Tyrosine sulfation enhances the chemokine binding affinity of N-terminal peptide fragments of receptors and influences various aspects of receptor activity.<sup>22,26,28</sup>

Based on the knowledge that sulfation of Tyr residues within the N-terminus of receptors is important for chemokine binding and that sulfate groups on GAGs also contribute to chemokine recognition,<sup>29-31</sup> we envisaged that a simplified molecule that displayed multiple sulfate or sulfonate moieties may be capable of recognising and binding to chemokines in solution with high affinity. A number of prior studies have focused on the synthesis of molecules possessing

<sup>a</sup> School of Chemistry, The University of Sydney, New South Wales 2006, Australia.

<sup>b</sup> Department of Biochemistry and Molecular Biology, Monash University, Melbourne, Victoria, Australia

<sup>c</sup> Department of Chemistry, University of Warwick, Coventry, CV4 7AL, United Kingdom

<sup>d</sup> Faculty of Pharmacy and Pharmaceutical Sciences, Monash University, 381 Royal Parade, Parkville, VIC 3052, Australia

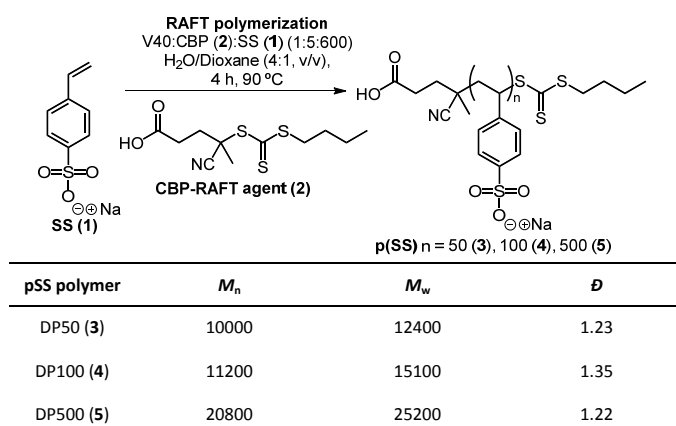
Electronic Supplementary Information (ESI) available: materials and methods, silica nanoparticle synthesis, NMR data and calculations. See DOI: 10.1039/x0xx00000x

polysulfonate groups for potential use as HIV therapies<sup>32</sup>. For example, it has been demonstrated that poly(styrene sulfonate) p(SS) polymers can efficiently bind to extracellular free forms of Tat and gp120 for inhibition of HIV-host cell interactions<sup>33</sup> and can inhibit HIV-1 cytopathicity<sup>34</sup>. The interaction between sulfated glycosylaminoglycans and the cationic V3 loop of gp120 of the HIV virus is known to be critical for infection.<sup>35</sup> This knowledge has led to the development of poly(naphthalene sulfonate) (PRO2000) as an anti-HIV polymer.<sup>36</sup> Herein, we report our efforts to develop chemokine-binding polystyrene sulfonate p(SS) polymer brushes as well as p(SS) polymer-brush derived silica nanoparticles with control of the length and number of sulfonate moieties. The binding of these polymers and polymer-derived nanoparticles to the chemokine monocyte chemoattractant protein-1 (MCP-1) was also investigated to assess the contribution of size and multivalency of the constructs on chemokine affinity.

## Results and discussion

### Synthesis of p(SS) polymers

p(SS) polymer brushes were synthesised from 4-styrene sulfonate sodium salt (SS) monomer **1** by reversible addition fragmentation chain transfer (RAFT) polymerisation using 4(((butylthio)carbonthioyl)thio)-4-cyanopentanoic acid (CBP) **2** as a chain transfer agent. Polymerisation reactions were carried out in a mixed solvent comprising water and dioxane at 90 °C in the presence of the azo-based radical initiator, V40 (1,1'-azobis(cyclohexane-1-carbonitrile)) (Scheme 1). These conditions led to controlled reactions and the generation of well-defined sulfonated polymers. Polymers with degree of polymerisation of 50 (**3**), 100 (**4**) and 500 (**5**) were prepared to a 50% monomer conversion before reactions were quenched (Scheme 1). Polymers **3-5** were characterised by aqueous size exclusion chromatography calibrated against polyethylene glycol/polyethylene oxide (PEG/PEO) standards and were shown to have a narrow dispersity ( $\bar{D}$ = 1.2-1.3, Scheme 1 and Figure 1).



**Scheme 1.** Synthesis of p(SS) polymers via RAFT and Table of  $M_n$ ,  $M_w$ , and dispersity of p(SS) polymers measured against PEG/PEO standards.

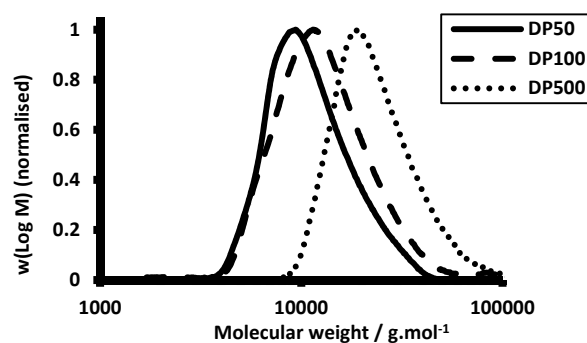


**Figure 1.** SEC chromatograms of poly(styrene sulfonate) in water calibrated against PEG/PEO standards.

### Synthesis of p(SS)-derived nanoparticles

Having successfully prepared p(SS) polymers with varying degrees of polymerisation, we next sought to synthesise silica nanoparticles modified with p(SS) brushes. Silica nanoparticles were synthesised using a modified Stöber synthesis protocol<sup>37</sup> and resulted in uniform particles with an average diameter of 100 nm [polydispersity Index, PDI = 0.003, as measured by dynamic light scattering (DLS), see Supplementary Information]. Functionalisation of these particles was next carried out with a chain transfer agent anchored to the particle surface by a triethoxysilane group (Scheme 2) that would enable surface-initiated polymerisation<sup>38, 39</sup> of p(SS) brushes. Triethoxysilane-functionalised CBP chain transfer agent **6** was first prepared by reacting **2** with (3-aminopropyl)triethoxysilane **7** in the presence of EDC and DMAP. Functionalisation of the particles was achieved by treatment of the particles with **7** in THF and dioxane to afford the RAFT agent functionalised particles (**8**). A grafting density of 0.967 RAFT agents/nm<sup>2</sup> of the particles was calculated from TGA experiments (See Supplementary Information).

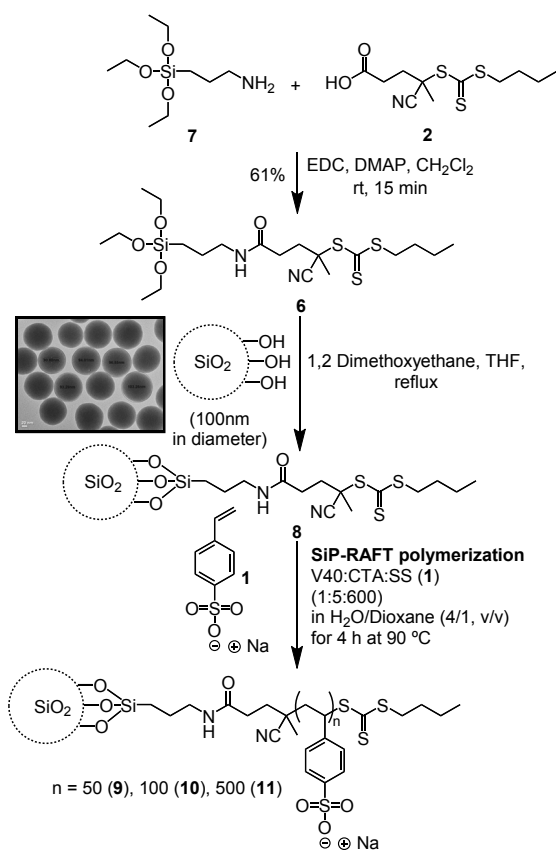
The RAFT agent functionalised particles were next used to mediate the radical polymerisation of styrene sulfonate **1**, using V40 as the thermal initiator in a mixture of dioxane and water and the reaction heated at 90 °C. Particles with polymer brushes with degree of polymerisation of 50 (**9**), 100 (**10**) and 500 (**11**) were targeted to enable a direct comparison with their free polymer equivalent. Using NMR the  $M_w$  of the polymer brushes in particles **9-11** were approximated by monomer conversion. We also used TGA to measure the polymer content on the various hybrid nanoparticles, as described for the characterisation of hybrid nanoparticles previously, which showed an increase in polymer content in going from polymer-derived particle **9** to **10** and from **10** to **11**.<sup>40</sup>

Dynamic Light Scattering (DLS) measurements of hydrodynamic particle diameters of 1 wt% of hybrid nanoparticles in solution were next performed in water and in 50 mM MOPS, the latter being the buffer system that we planned to use in the chemokine binding assays. The polymer brush heights of the final particles were calculated according to (equation 1) and are shown in Table 1.

$$h = \frac{(D_h - D_o)}{2} \quad (\text{eq. 1})$$

where  $h$  is the brush height,  $D_h$  the hydrodynamic diameter of hybrid particles and  $D_o$  the hydrodynamic diameter of bare silica nanoparticles.

DLS measurements in water and in buffer show that an increase in ionic strength of the solution causes the polyelectrolyte brushes to coil and collapse at the surface of the particles (Table 1). Specifically, in 50 mM MOPS buffer, polymer brushes have a reduced hydrodynamic diameter and polydispersity (Pdl) compared to the same particles in water.



**Scheme 2.** Synthesis of p(SS) functionalised silica nanoparticles. Inset: TEM image of 100 nm silica nanoparticles synthesised via a modified Stöber method (see Supplementary Information for enlarged image with scale bar).

We also measured the zeta potential and electrophoretic mobility of polymer-derived particles **9-11** in order to gauge the amount of negative charge on the surface of the particles (Table 2). Interestingly, a decrease in net negative charge and electrophoretic mobility of the particles was observed with increasing polymer content which suggests some of the charges may be buried within the brush when the polymer chains get longer.<sup>41</sup>

**Table 1:** DLS characterisation of 1 wt% of hybrid nanoparticles in solution

p(SS) derived particles	Water		50mM MOPS	
	Size (Brush Height) [nm]	Pdl	Size (Brush Height) [nm]	Pdl
DP 50 ( <b>9</b> )	263.5 (70.6)	0.234	196.5 (37.1)	0.016
DP 100 ( <b>10</b> )	262.8 (70.3)	0.028	229.1 (53.4)	0.018
DP 500 ( <b>11</b> )	268.6 (73.2)	0.021	244.1 (60.9)	0.018

**Table 2:** Zeta potential measurements of 1 wt% of hybrid nanoparticles in water

p(SS) derived particles	Zeta potential (mV)	Electrophoretic Mobility ( $\mu\text{cm}^2/\text{Vs}$ )
DP 50 ( <b>9</b> )	-55.7	-4.37
DP 100 ( <b>10</b> )	-46.0	-3.60
DP 500 ( <b>11</b> )	-44.7	-3.50

Taken together, the data suggest that the unique hybrid structures prepared in this study result in concentrated polymer brush regimes on the surface of the silica nanoparticles (Figure 2). This is most probably owing to the high grafting density (0.967 chains/nm<sup>2</sup>) as well as the polyanionic nature of the brushes.<sup>42, 43</sup>

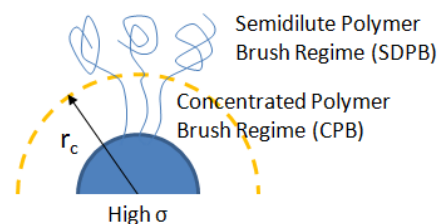


**Figure 2.** Polymer brush configurations on curved surfaces

### Binding affinities of p(SS) polymers and p(SS) polymer-derived particles to the chemokine MCP-1

We have recently reported the development of a fluorescence anisotropy-based assay to determine the affinities of chemokines for receptor-derived peptides containing sulfated Tyr residues.<sup>44</sup> In this study the assay was adapted to investigate the binding affinity of MCP-1 for p(SS) polymers **3-5** and p(SS)-derived particles **9-11**. Briefly, the chemokine was incubated with a fluorescent receptor-derived sulfopeptide in the presence of various concentrations of the polymers or nanoparticles. As the concentration was increased, the fluorescent peptide was displaced from the chemokine, resulting in decreased fluorescence anisotropy (Figure 3). This binding assay was used to study the interactions of an obligate monomeric mutant (P8A) and obligate dimeric mutant (T10C) of the chemokine. We have previously shown that MCP-1(P8A), which is unable to dimerise, has the ability to activate the chemokine receptor CCR2 *in vitro*. In contrast, MCP-1(T10C), which is trapped in the dimeric state by a disulfide bond, is unable to elicit activation of CCR2 *in vitro* but still binds to sulfopeptides derived from CCR2.<sup>26, 45</sup> Here, we used these two different forms of the chemokine to

obtain insights into the structural basis of binding to p(SS) polymers and particles, including the potential contribution of multivalency.

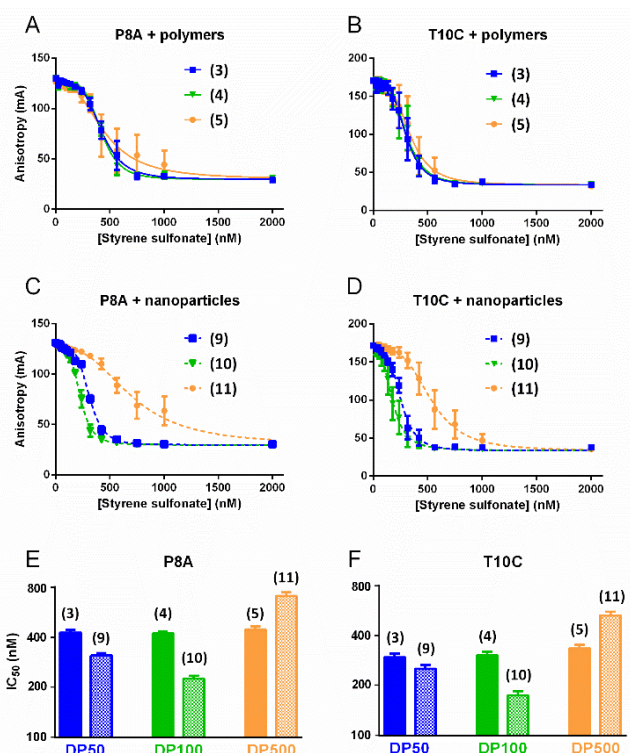


**Figure 3.** Fluorescence anisotropy per styrene sulfate monomer of A) p(SS) polymers **3**, **4** and **5** with MCP-1(P8A); B) polymers **3**, **4** and **5** with MCP-1(T10C); C) p(SS)-derived particles **9**, **10** and **11** with MCP-1(P8A); and D) p(SS)-derived particles **9**, **10** and **11** with MCP-1(T10C). E) and F) represent the IC<sub>50</sub> values for binding to MCP-1(P8A) and MCP-1(T10C), respectively. The anisotropy signal was measured in milli-anisotropy units (mA) and the data displayed are the averages of three independent experiments with error bars representing the SEM.

The free p(SS) polymers **3-5** with various degrees of polymerisation, were first assessed for their binding to MCP-1(P8A) and MCP-1(T10C) (Figure 3A and 3B). Fluorescence anisotropy was plotted with respect to styrene sulfonate concentration and fitted to yield the concentration at which binding is 50% inhibited (IC<sub>50</sub>), representing the apparent affinity of the polymer for the chemokine (Figure 3E and 3F). Gratifyingly, each of the polymers showed significant binding to the MCP-1 variants. However, there was no discernible difference in IC<sub>50</sub> values, suggesting that chemokine binding sites on all three polymers are similar and that MCP-1 binds to p(SS) polymers in a non-cooperative manner. Moreover, the similar affinities of both monomeric and dimeric MCP-1 to p(SS) polymers indicated that the p(SS) binding site is on the exposed surface of the dimer, suggesting it may be the same as the binding site for the sulfotyrosine moieties of CCR2.<sup>22, 26, 28</sup>

When these studies were translated to a particle configuration (**9-11**), significant differences in binding affinity were observed for particles bearing different chain length polymers (Figure 3C-F). Particles **9** and **10**, bearing DP50 and DP100 polymer brushes, respectively, had the highest apparent affinities to the chemokines and outperformed the binding observed for the free polymer

counterparts (**3** and **4**). These increased affinities could potentially be due to the higher negative charge density on the nanoparticles than the polymers, thus more strongly attracting the positively charged chemokines, or to reduced solvent screening on the nanoparticle surface than on polymers in solution. Alternatively, the loss of polymer chain entropy upon chemokine binding may be lower in the structurally constrained environment of a nanoparticle. In contrast to the DP50 and DP100 nanoparticles, the nanoparticles bearing DP500 polymer brushes (**11**) bound to chemokines more weakly (per styrene sulfonate) than the corresponding free polymers and substantially more weakly than shorter brush length nanoparticles (Figure 3C-F). Although it is possible that the particles with shorter brushes contain binding sites with higher microscopic affinities or that there is positive cooperativity between binding sites only in the shorter polymers (or negative cooperativity only in the longer polymers), considerations of nanoparticle structure suggest an alternative explanation. As shown in Table 1, the brush height of DP500 particles (**11**) is not significantly different to that of DP100 (**10**) despite the 400% increase in chain length. This indicates that the chains of the DP500 particles are folded back onto the silica core. The zeta potential of the polyelectrolyte brushes also decreases with increased polymer content, thus suggesting that charged groups might be confined within the brush, and therefore, the number of available binding sites per styrene sulfonate group is likely to be lower than for the shorter chain length particles. These observations suggest a significant correlation between brush heights and sites of interaction which indicates that for a silica core of 100 nm with a grafting density of 0.967 chains/nm<sup>2</sup>, the brush lengths of DP 50 and 100 are the most appropriate for chemokine binding. We postulate that the weaker apparent binding affinity of the DP500 particles is a manifestation of the lower concentration of binding-competent styrene sulfonate groups in the relatively condensed brushes of these long-chain nanoparticles.

## Conclusions

In summary, we have utilised RAFT polymerisation to generate polymers possessing different numbers of styrene sulfonate moieties which were designed to mimic sulfated Tyr residues found on the N-terminal extracellular domain of chemokine receptors. We have also employed surface-initiated RAFT polymerisation to synthesise well defined hybrid silica nanoparticles modified with dense p(SS) brushes that possess a corona of sulfonate groups on the surface. While both the p(SS) polymers and p(SS)-derived particles were shown to bind to two variants of the chemokine MCP-1 with high affinity, the shorter chain length particles demonstrated tighter binding per styrene sulfonate group whereas longer chain length particles demonstrated weaker binding in comparison to the corresponding non-constrained polymers. This work indicates that constraining p(SS) polymers on nanoparticles alters their chemokine binding properties and lays the foundation for the development of particles that possess selectivity for specific chemokines and have valuable therapeutic or diagnostic applications.

## Experimental

## Synthesis of free poly(styrene sulfonate) (p(SS))

Polymerisation of styrene sulfonate sodium salt (SS, **1**) was carried out with V40 as the initiator and CBP (**2**) as the controlled transfer agent. Concentrations of SS (**1**), V40 and CBP (**2**) (Table 2) were added to a mixed solvent comprising 4/1, v/v water/dioxane in a round bottomed flask equipped with a magnetic stirrer. A sample of the reaction was taken for  $^1\text{H-NMR}$  analysis at  $t = 0$ . The reaction was then degassed with pure nitrogen for 20 minutes before allowing heating at  $90^\circ\text{C}$  for 4 h. Reactions were monitored by  $^1\text{H-NMR}$  for monomer conversion which was calculated with respect to the  $t = 0$  sample.

**Table 2.** Polymerisation conditions for p(SS)

Samples	Concentration		
	[SS] (M)	[CBP-RAFT] (mM)	[V40] (mM)
p(SS) <sub>50</sub>	1	8.0	1.6
p(SS) <sub>100</sub>	1	4.2	0.83
p(SS) <sub>500</sub>	1	0.8	0.16

For a degree of polymerisation of 50 (DP50) the reaction was carried out with a 1:5:600 (initiator:CTA:monomer molar concentration ratio). The ratio was changed to 1:5:1200 and 1:5:6000 for DP100 and DP500 samples, respectively. Polymer solutions were quenched by air to stop the reaction after 50% monomer conversion to reduce the amount of dead polymer chains. p(SS) polymers were dialysed in 2 kDa dialysis tubing against MilliQ water overnight and freeze dried to a yellow powder.

4(((Butylthio)carbonthioly)thio)-4-cyanopentanoic acid (CBP-RAFT agent) **2**

CPB RAFT agent **2** was synthesised via a modified procedure to that previously reported by Moad et al.<sup>46</sup> 1-Butanethiol (18 g, 0.2 mol) was added dropwise to a solution of potassium hydroxide (14 g, 0.25 mol) in water (70 mL) and allowed to stir for 30 minutes. Carbon disulfide (31 g, 0.4 mol) was then added to the reaction which was stirred for an additional 40 min. *p*-Tosyl chloride (19 g, 0.1 mol) in acetone (110 mL) was added portionwise and the reaction stirred for 2 h. The solvent was concentrated under reduced pressure before redissolving the resulting residue in  $\text{CH}_2\text{Cl}_2$  (100 mL), washed with water (3 x 100 mL) and dried over magnesium sulfate. Purification by flash column chromatography (eluent: hexane) gave the disulfide intermediate as a red oil (28 g, 66%). A solution of the disulfide intermediate (3.5 g, 10 mmol) and 4,4'-azobis(4-cyanovaleric acid) (3.5 g, 13  $\mu\text{mol}$ ) in ethyl acetate (50 mL) was heated under reflux for 20 h. Purification by column chromatography (eluent: hexane/ethyl acetate 1/1, v/v) gave RAFT agent **2** as a yellow oil (5.8 g, 85%).  $^1\text{H-NMR}$  (300 MHz,  $\text{CDCl}_3$ )  $\delta$ ppm: 0.95 (t, 3H,  $J = 7.68$  Hz,  $\text{CH}_3\text{-CH}_2\text{-CH}_2$ ), 1.36-1.58 (m, 2H,  $\text{CH}_3\text{-CH}_2\text{-CH}_2$ ), 1.59-1.78 (m, 2H,  $\text{CH}_3\text{-CH}_2\text{-CH}_2$ ), 1.89 (s, 3H, S-C- $\text{CH}_3$ ), 2.24-2.83 (m, 6H,  $\text{CH}_3\text{-CH}_3\text{-COOH}$ ), 3.20-3.48 (m, 2H,  $\text{CH}_2\text{-CH}_2\text{-CH}_2\text{-S}$ );  $^{13}\text{C-NMR}$  (300MHz,  $\text{CDCl}_3$ )  $\delta$  ppm: 13.6, 22.1, 24.8, 29.7, 33.5,

36.8, 46.2, 118.9, 176.5, 216.8. LRMS: ESI (M+H)<sup>+</sup> 292.1. These data are in agreement with those previously reported by Moad et al.<sup>46</sup>

## Functionalisation of CBP-RAFT agent with triethoxysilane

CBP-RAFT agent **2** (2.0 g, 7 mmol) was dissolved in  $\text{CH}_2\text{Cl}_2$  (5 mL) and cooled in an ice bath for 30 min. 4-(Dimethylamino)pyridine (0.10 g, 8.0 mmol) and *N*-(3-Dimethylaminopropyl)-*N'*-ethylcarbodiimide hydrochloride (1.6 g, 8.0 mmol) were dissolved in  $\text{CH}_2\text{Cl}_2$  (5 mL) before adding dropwise to the CBP-RAFT agent solution prepared above. Finally, (3-aminopropyl)triethoxysilane **7** (1.9 g, 8.0 mmol) was added to the reaction mixture and the reaction stirred at rt for 16 h. The crude product was purified by column chromatography on silica gel (eluent: hexane/ethyl acetate 1/1, v/v) to afford **6** as a yellow oil (1.9 g, 61%).  $^1\text{H-NMR}$  (300 MHz,  $\text{CDCl}_3$ )  $\delta$  ppm: 1.18-1.33 (t, 9H,  $J = 7.0$ ,  $\text{CH}_3\text{-CH}_2\text{-O-Si}$ ), 3.74-3.95 (m, 6H,  $\text{CH}_3\text{-CH}_2\text{-O-Si}$ ), 0.50-0.75 (m, 2H, Si- $\text{CH}_2\text{-CH}_2\text{-CH}_2$ ), 1.55-1.75 (m, 2H, Si- $\text{CH}_2\text{-CH}_2\text{-CH}_2$ ), 3.15-3.50 (m, 2H, Si- $\text{CH}_2\text{-CH}_2\text{-CH}_2$ ), 5.80-6.10 (brs, 1H,  $\text{CH}_2\text{-NH-CO}$ ), 2.25-2.70 (m, 4H, CO- $\text{CH}_2\text{-CH}_2$ ), 1.89 (s, 3H, S-C- $\text{CH}_3$ ), 3.20-3.50 (m, 2H, S- $\text{CH}_2\text{-CH}_2\text{-CH}_2\text{-CH}_3$ ), 1.55-1.75 (m, 2H, S- $\text{CH}_2\text{-CH}_2\text{-CH}_2\text{-CH}_3$ ), 1.30-1.50 (m, 2H, S- $\text{CH}_2\text{-CH}_2\text{-CH}_2\text{-CH}_3$ ), 0.80-1.10 (t, 3H,  $J = 8.4$  Hz, S- $\text{CH}_2\text{-CH}_2\text{-CH}_2\text{-CH}_3$ );  $^{13}\text{C-NMR}$  (300MHz,  $\text{CDCl}_3$ )  $\delta$  ppm: 13.4, 18.1, 21.3, 24.6, 29.5, 31.0, 36.2, 38.5, 46.5, 53.3, 119.0, 170.1, 217.1.

## Synthesis of functionalised silica particles for surface initiated polymerisation

Silica particles prepared by the modified Stöber protocol<sup>37</sup> (1.1 g) were centrifuged (14000 rpm for 20 min) to remove excess EtOH and redispersed in 1,2 dimethoxyethane (46 mL) followed by addition of triethoxysilane-CBP **6** (1.9 g, 4.2 mmol) in THF (4 mL). The reaction mixture was heated at  $95^\circ\text{C}$  with constant stirring for 16 h. Particles were then collected *via* centrifugation at 14000 rpm for 20 min. The particles were then washed with EtOH (2 x 10 mL), acetone (2 x 10 mL), toluene (2 x 10 mL) and DMF (4 x 10 mL) before finally dispersing them in DMF (10 mL) for storage. Functionalised particles were characterised for using TGA (See Supplementary Information).

Synthesis of SiP-p(SS) *via* surface initiated RAFT polymerisation

3.9 g of 14% w/w of SiP-CBP functionalised silica nanoparticles in DMF (Supplementary Information) were centrifuged to a pellet and the DMF was removed (0.6 g of SiP-CBP functionalised particles, approx. 0.4  $\mu\text{mol}$  of CBP-RAFT). The particles were then resuspended in a mixture of 0.01vol.% V40 in dioxane (200  $\mu\text{L}$ ), styrene sulfonate sodium salt (10 mg, 40  $\mu\text{mol}$ ) and milliQ water (800  $\mu\text{L}$ ) by 30 sec of ultrasonication followed by vortex mixing. The reaction mixture was then degassed with argon for 10 min before heating at  $90^\circ\text{C}$  in an oil bath for 6.5 h. The molar concentration ratio of initiator:CTA:monomer were maintained as the free p(SS) polymer samples. The reaction was stopped once it has reached a

monomer conversion of 50% (approximated from free polymer syntheses). Particles were then centrifuged and washed with water/dioxane solvent mixture (4/1, v/v) 3 times and with milliQ water before storing as a colloidal suspension in milliQ water to give a final concentration of 1 wt% of particles in solution.

#### Fluorescence anisotropy assays for binding of proteins

Competitive fluorescence anisotropy assays were performed at 25 °C using Greiner nonbinding, black, flat-bottomed, 384-well microplates (catalogue no. 781900) and a BMG Labtech PHERAstar FS plate reader equipped with a fluorescence polarisation module with dedicated excitation and emission wavelengths of 485 and 520 nm, respectively. Samples contained the fluorescein-labelled chemokine receptor-derived sulfopeptide FL-R2D described previously<sup>44</sup> (final concentration 10 nM), MCP-1(P8A or T10C) produced as described previously<sup>45</sup> (final concentration 100 nM), and serially 1.33-fold diluted p(SS) polymers **3-5** or p(SS)-derived nanoparticles **9-11**, ranging in styrene sulfonate concentration from 2.0 μM to 23.8 nM. All competitive binding assays were performed in 50 mM MOPS, pH 7.0 with final sample volumes of 60 μL in each well. Duplicate assays were performed three times independently and the average data fitted by non-linear regression analysis using GraphPad Prism v.6.0 software to the equation for a sigmoidal dose-response with variable slope in which: the independent variable is the concentration of styrene sulfonate moieties; the dependent variable is the observed anisotropy signal; and fitted parameters are the shared initial and final anisotropy signal, the Hill slope and the IC<sub>50</sub> value (per styrene sulfonate moiety) for binding of the p(SS) polymers or p(SS)-derived nanoparticles MCP-1(P8A or T10C).

#### Acknowledgements

The authors would like to acknowledge funding from an Australian Postgraduate Award (NI), Monash International Postgraduate Research Scholarship and Monash Graduate Scholarship (JS), the Australian Research Council (RJP, Future Fellowship FT130100150) and Discovery Project grant (DP130101984, RJP and MJS), the Royal Society Wolfson Merit Award (WM130055; SP) and the Monash-Warwick Alliance (SP).

#### References

1. A. Ben-Baruch, D. F. Michiel and J. J. Oppenheim, *J. Biol. Chem.*, 1995, **270**, 11703-11706.
2. A. Muller, B. Homey, H. Soto, N. F. Ge, D. Catron, M. E. Buchanan, T. McClanahan, E. Murphy, W. Yuan, S. N. Wagner, J. L. Barrera, A. Mohar, E. Verastegui and A. Zlotnik, *Nature*, 2001, **410**, 50-56.
3. M. Farzan, T. Mirzabekov, P. Kolchinsky, R. Wyatt, M. Cayabyab, N. P. Gerard, C. Gerard, J. Sodroski and H. Choe, *Cell*, 1999, **96**, 667-676.
4. H. Choe, M. J. Moore, C. M. Owens, P. L. Wright, N. Vasilieva, W. Li, A. P. Singh, R. Shakri, C. E. Chitnis and M. Farzan, *Mol. Microbiol.*, 2005, **55**, 1413-1422.
5. R. Horuk, *Nat. Rev. Drug Discov.*, 2009, **8**, 23-33.
6. A. E. I. Proudfoot, *Nat. Rev. Immunol.*, 2002, **2**, 106-115.
7. J. Pearce and R. Horuk, *J. Med. Chem.*, 2012, **55**, 9363-9392.
8. E. De Clercq and D. Schols, *Antivir. Chem. Chemother.*, 2001, **12**, 19-31.
9. M. O'Hayre, C. L. Salanga, T. M. Handel and D. J. Hamel, *Expert Opin. Drug Discov.*, 2010, **5**, 1109-1122.
10. P. Dorr, M. Westby, S. Dobbs, P. Griffin, B. Irvine, M. Macartney, J. Mori, G. Rickett, C. Smith-Burchnell, C. Napier, R. Webster, D. A. D. Price, B. Stammen, A. Wood and M. Perros, *Antimicrob. Agents Chemother.*, 2005, **49**, 4721-4732.
11. S. Main, R. Handy, J. Wilton, S. Smith, L. Williams, L. D. Fou, J. Andrews, L. A. Conroy, R. May, I. Anderson and T. J. Vaughan, *J. Pharmacol. Exp. Ther.*, 2006, **319**, 1395-1404.
12. C. Ding, J. Li and X. Zhang, *Curr. Opin. Investig. Drugs*, 2004, **5**, 1213-1218.
13. C. Bizzarri, A. R. Beccari, R. Bertini, M. R. Cavicchia, S. Giorgini and M. Allegretti, *Pharmacol. Ther.*, 2006, **112**, 139-149.
14. L. Kincaid, *Drug Discov. Today*, 2005, **10**, 884-886.
15. I. Clark-Lewis, C. Schumacher, M. Baggiolini and B. Moser, *J. Biol. Chem.*, 1991, **266**, 23128-23134.
16. M. P. Crump, J. H. Gong, P. Loetscher, K. Rajarathnam, A. Amara, F. Arenzana-Seisdedos, J. L. Virelizier, M. Baggiolini, B. D. Sykes and I. Clark-Lewis, *EMBO J.*, 1997, **16**, 6996-7007.
17. C. T. Veldkamp, C. Seibert, F. C. Peterson, N. B. De la Cruz, J. C. Haugner, 3rd, H. Basnet, T. P. Sakmar and B. F. Volkman, *Sci. Signal.*, 2008, **1**, ra4.
18. J. Ye, L. L. Kohli and M. J. Stone, *J. Biol. Chem.*, 2000, **275**, 27250-27257.
19. C. J. Millard, J. P. Ludeman, M. Canals, J. L. Bridgford, M. G. Hinds, D. J. Clayton, A. Christopoulos, R. J. Payne and M. J. Stone, *Structure*, 2014, **22**, 1571-1581.
20. L. Qin, I. Kufareva, L. G. Holden, C. Wang, Y. Zheng, C. Zhao, G. Fenalti, H. Wu, G. W. Han, V. Cherezov, R. Abagyan, R. C. Stevens and T. M. Handel, *Science*, 2015, **347**, 1117-1122.
21. J. S. Burg, J. R. Ingram, A. J. Venkatakrishnan, K. M. Jude, A. Dukkupati, E. N. Feinberg, A. Angelini, D. Waghray, R. O. Dror, H. L. Ploegh and K. C. Garcia, *Science*, 2015, **347**, 1113-1117.
22. M. J. Stone and R. J. Payne, *Acc. Chem. Res.*, 2015, **48**, 2251-2261.
23. J. J. Ziarek, A. E. Getschman, S. J. Butler, D. Taleski, B. Stephens, I. Kufareva, T. M. Handel, R. J. Payne and B. F. Volkman, *ACS Chem. Biol.*, 2013, **8**, 1955-1963.
24. J. Z. Zhu, C. J. Millard, J. P. Ludeman, L. S. Simpson, D. J. Clayton, R. J. Payne, T. S. Widlanski and M. J. Stone, *Biochemistry*, 2011, **50**, 1524-1534.
25. J. P. Ludeman and M. J. Stone, *Brit. J. Pharmacol.*, 2014, **171**, 1167-1179.
26. J. Liu, S. Louie, W. Hsu, K. M. Yu, H. B. Nicholas and G. L. Rosenquist, *American J. Respir. Cell Mol. Biol.*, 2008, **38**, 738-743.
27. M. J. Stone, S. Chuang, X. Hou, M. Shoham and J. Z. Zhu, *N. Biotechnol.*, 2009, **25**, 299-317.
28. J. H. Y. Tan, J. P. Ludeman, J. Wedderburn, M. Canals, P. Hall, S. J. Butler, D. Taleski, A. Christopoulos, M. J. Hickey,

- R. J. Payne and M. J. Stone, *J. Biol. Chem.*, 2013, **288**, 10024-10034.
29. G. S. Kuschert, F. Coulin, C. A. Power, A. E. Proudfoot, R. E. Hubbard, A. J. Hoogewerf and T. N. Wells, *Biochemistry*, 1999, **38**, 12959-12968.
30. D. P. Witt and A. D. Lander, *Curr. Biol.*, 1994, **4**, 394-400.
31. D. P. Dyer, C. L. Salanga, B. F. Volkman, T. Kawamura and T. M. Handel, *Glycobiology*, 2015, DOI: 10.1093/glycob/cwv100.
32. M. Rusnati, P. Oreste, G. Zoppetti and M. Presta, *Curr. Pharm. Des.*, 2005, **11**, 2489-2499.
33. A. Bugatti, C. Urbinati, C. Ravelli, E. De Clercq, S. Liekens and M. Rusnati, *Antimicrob. Agents Chemother.* 2007, **51**, 2337-2345.
34. P. Mohan, D. Schols, M. Baba and E. De Clercq, *Antivir. Res.*, 1992, **18**, 139-150.
35. D. Batinić and F. A. Robey, *J. Biol. Chem.*, 1992, **267**, 6664-6671.
36. M. Danial and H.-A. Klok, *Macromol. Biosci.*, 2015, **15**, 9-35.
37. W. Stöber, A. Fink and E. Bohn, *J. Coll. Interface Sci.*, 1968, **26**, 62-69.
38. K. Ohno, Y. Ma, Y. Huang, C. Mori, Y. Yahata, Y. Tsujii, T. Maschmeyer, J. Moraes and S. Perrier, *Macromolecules*, 2011, **44**, 8944-8953.
39. J. Moraes, K. Ohno, G. Gody, T. Maschmeyer and S. Perrier, *Beilstein J. Org. Chem.*, 2013, **9**, 1226-1234.
40. J. Moraes, K. Ohno, T. Maschmeyer and S. Perrier, *Chem. Commun.*, 2013, **49**, 9077-9088.
41. J. Irigoyen, V. B. Arekalyan, Z. Navoyan, J. Iturri, S. E. Moya and E. Donath, *Soft Matter*, 2013, **9**, 11609-11617.
42. D. Dukes, Y. Li, S. Lewis, B. Benicewicz, L. Schadler and S. K. Kumar, *Macromolecules*, 2010, **43**, 1564-1570.
43. K. Ohno, T. Morinaga, S. Takeno, Y. Tsujii and T. Fukuda, *Macromolecules*, 2007, **40**, 9143-9150.
44. J. P. Ludeman, M. Nazari-Robati, B. L. Wilkinson, C. Huang, R. J. Payne and M. J. Stone, *Org. Biomol. Chem.*, 2015, **13**, 2162-2169.
45. J. H. Y. Tan, M. Canals, J. P. Ludeman, J. Wedderburn, C. Boston, S. J. Butler, A. M. Carrick, T. R. Parody, D. Taleski, A. Christopoulos, R. J. Payne and M. J. Stone, *J. Biol. Chem.*, 2012, **287**, 14692-14702.
46. G. Moad, Y. K. Chong, A. Postma, E. Rizzardo and S. H. Thang, *Polymer*, 2005, **46**, 8458-8468.